

Multi-Task Learning from Videos via Efficient Inter-Frame Attention

Donghyun Kim¹, Tian Lan², Chuhan Zou², Ning Xu²,
 Bryan A. Plummer¹, Stan Sclaroff¹, Jayan Eledath², Gerard Medioni²
¹Boston University, ² Amazon

¹{donhk, bplum, sclaroff}@bu.edu, ²{tianlan, ninxu, zouchuha, eledathj, medioni}@amazon.com

Abstract

Prior work in multi-task learning has mainly focused on predictions on a single image. In this work, we present a new approach for multi-task learning from videos. Our approach contains a novel inter-frame attention module which allows learning of task-specific attention across frames. We embed the attention module in a “slow-fast” architecture, where the slower network runs on sparsely sampled key frames and the lightweight shallow network runs on non-key frames at a high frame rate. We further propose an effective adversarial learning strategy to encourage the slow and fast network to learn similar features. The proposed architecture ensures low-latency multi-task learning while maintaining high quality prediction. Experiments show competitive accuracy compared to state-of-the-art on two multi-task learning benchmarks while reducing the number of floating point operations (FLOPs) by 70%. Meanwhile, our attention based feature propagation outperforms other feature propagation methods in accuracy by up to 90% reduction of FLOPs.

1. Introduction

Computer vision applications, such as autonomous driving and indoor navigation, require multi-task predictions from video streams. For example, a self-driving system needs semantic segmentation at each time frame to understand what entities are around the car, and depth estimation to determine how far away each entity is. In this case, multi-task learning is more favoured given the advantages of simultaneous inference that reduces computation cost, and a shared representation that boosts performance for each task.

In this paper, we focus on multi-task learning for dense pixel-wise predictions (e.g. semantic segmentation and depth estimation) from a monocular video. Recent multi-task learning approaches for dense predictions are mainly single frame based [13, 27, 30, 22], or a concatenation of the features from two consecutive frames from a video [4]. Different from previous approaches, we propose to exploit tem-

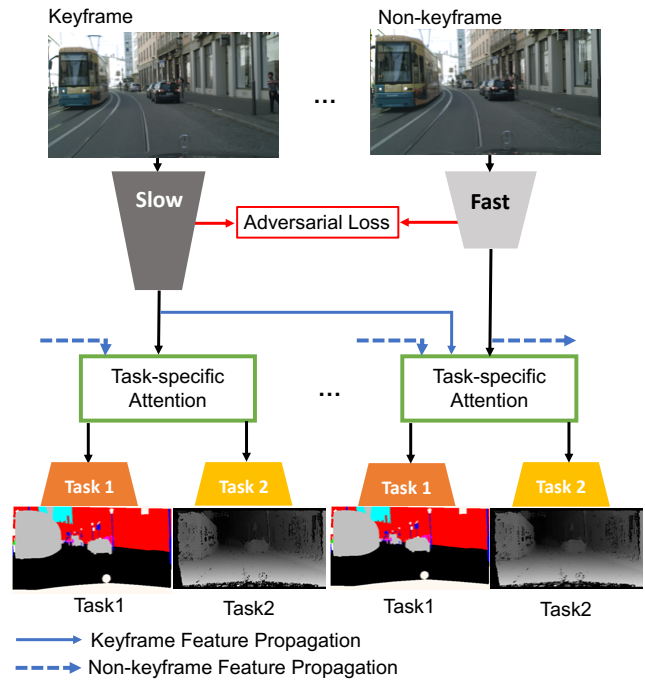


Figure 1: **Overview.** Given a video stream of RGB monocular images, we propose an efficient approach for multi-task pixel-wise predictions (semantic segmentation and depth estimation in this figure). Our method improves upon the SlowFast network due to a task-specific inter-frame attention module that exploits temporal cues, and an adversarial loss that improves the feature quality of the *Fast* network by mimicking the *Slow* network, which leads to improved prediction accuracy with low computational cost.

poral cues using inter-frame local attention modules. Different from existing attention modules in multi-task learning that propagate features in the current frame, our attention module learns to propagate features from the previous frames. Our attention module is light-weight as compared to the expensive optical flow based feature warping which is widely used in previous works [21, 40]. In addi-

tion, the performance of optical flow warping based methods can be affected by the quality of estimated optical flow, which may fail on fast motion or occluded objects. Our network architecture stems from the idea of the SlowFast network [21, 10], which shows superiority in reducing computational cost while maintaining comparable accuracy. In the SlowFast scheme, keyframes are processed by a deep (*Slow*) network, and non keyframes are processed by a shallow (*Fast*) network. We show improvements in accuracy with our task-specific attention based feature propagation, and a novel adversarial learning strategy that encourages similar feature representations for both the slow and fast network. Figure 1 illustrates our approach.

We evaluate our approach on two standard multi-task learning benchmarks: Cityscapes [5] dataset with outdoor scenes and NYUd v2 [34] dataset with indoor scenes. Our method achieves on-par accuracy compared to the state-of-the-art multi-task learning methods, while reducing the number of floating point operations (FLOPs) by 70%. Moreover, we show that our inter-frame local attention (ILA) module can be used as a standalone feature propagation method in videos: it is much faster compared to existing feature propagation methods, and more accurate than the state-of-the-art [21, 26] on semantic video segmentation.

Our contributions are :

- We address the task of video-based multi-task learning, which is not well explored in previous work. We present a framework that achieves competitive accuracy as compared to the state-of-the-art with largely reduced computational cost.
- We introduce a new inter-frame local attention module (ILA) which learns task-specific features across frames. Our network is trained end-to-end with an adversarial loss.
- Our ILA module can be used as a standalone feature propagation method in video tasks such as semantic segmentation, achieving the top accuracy with up to 90% reduction of FLOPs.

2. Related Work

Multi-task learning (MTL) has shown improved accuracy and increased memory-efficiency for various tasks such as object detection and segmentation [1, 2, 17, 30], joint scene geometry and semantic segmentation [4, 27, 38, 22, 35, 24, 9]. Previous approaches mainly focus on predictions from a single image. Chennupati *et al.* [4] propose to learn from videos by concatenating the features from two consecutive frames. Different from the previous work, we go beyond single-frame based prediction and learn from

videos by aggregating and propagating features across multiple frames.

Although the shared representation of MTL can help improve generalization and reduce computational costs, it is also shown to potentially hurt accuracy due to the trade-off learning from multiple tasks [29]. Kendall *et al.* [22] propose to use homoscedastic uncertainty to weight different tasks adaptively during training. Senser and Koltun [33] propose to optimize an upper bound for the multi-objective loss. However, refining the training loss usually has limited improvements. Other methods introduce complex task-specific layers (*e.g.* task-specific backbone) [27, 30, 32] but also increase the computational burden. Instead, we show that a task-specific design for our inter-frame attention module is able to achieve competitive results in accuracy while maintaining a much lower computational cost in experiments.

Feature propagation has been widely used in video applications to exploit temporal cues across frames [21, 26, 31, 40, 12]. Prior work has introduced methods based on optical flow based warping [40, 21, 12] which largely increases the computational cost with limited improvements in accuracy. Jain *et al.* [21] propose to reduce the inference cost by combining the predictions of two network branches: a deep reference branch that computes detailed features from keyframes, and a shallower update branch that incorporates less detailed features at each frame with the wrapped features from a recently met keyframe. This has the same spirit as the SlowFast [10] design for video recognition. Li *et al.* [26] further propose a dynamic keyframe selection strategy and use additional convolution layers to substitute optical flow to reduce latency. Our network architecture stems from the spirit of the SlowFast network, and we use our light-weight attention module for feature propagation instead of the expensive optical flow based approach. Moreover, we perform dense feature propagation between every neighboring frame, in addition to the sparse propagation between keyframes and non-keyframes only.

Attention modules are widely used in various tasks such as natural language processing (NLP) [7, 36], semantic segmentation [20, 25, 36, 11, 39], image classification [19, 37] and action recognition [15, 14]. Vaswani *et al.* [36] propose a self-attention module for a translation task by extracting global dependencies from input sequences. The self-attention first computes feature representations for query, key, and value, then computes global attention weights by measuring the similarity between the query and key. The final value can be obtained by a weighted sum of values from the sequence of input. Fu *et al.* [11] apply the self-attention module for semantic segmentation by attending all pixels given a pixel query in order to capture global relation in a single frame. We reformulate the self-attention mechanism to attend inter-frames from the two different representations

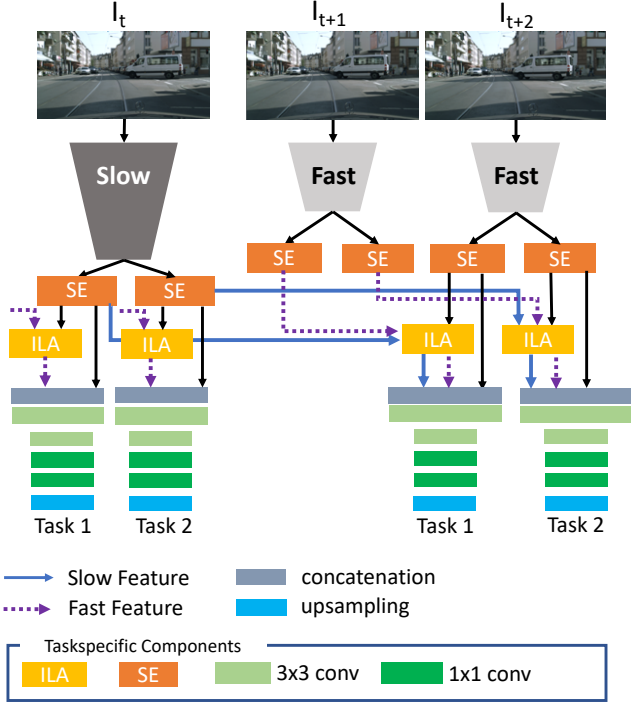


Figure 2: Architecture Overview. This figure illustrates our network architecture and the inference step of a keyframe I_t and a non-keyframe I_{t+2} .

(from *Slow* and *Fast* network) for efficient and accurate feature propagation.

3. Approach

Our goal is to have a low-latency multi-task learning model with high quality prediction on video streams. One major challenge is to effectively learn spatial and temporal cues of different tasks in a light-weight manner. Inspired by the SlowFast network [10, 21], we build an efficient multi-task network with a two-branch design: the “slow” branch runs on sparsely sampled key frames and the light-weight fast network runs on non-key frames. We introduce a new task-specific attention module to learn and propagate task-specific features across frames.

In the following, we first explain our multi-task network architecture (Sec. 3.1). Then, we introduce our novel task-specific inter-frame local attention (ILA) module (Sec. 3.2), and an adversarial loss that further boosts the overall performance (Sec. 3.3).

3.1. Architecture Overview

Our multi-task network consists of two components: 1) a shared encoder network: a *Slow* network that operates on sparsely sampled keyframes; a *Fast* network runs on other frames. 2) M task-specific decoder networks, one for each

task. Each decoder network learns to attend to task-specific features from previous frames, propagate the features across frames and perform pixel-level prediction of the task labels.

Figure 2 shows the architecture of the proposed network. The input is a sequence of N RGB frames $I = \{I_1, I_2, \dots, I_N\}$ from a monocular video, and the output is pixel-level predictions on M tasks, $Y = \{y_1, y_2, \dots, y_M\}$. At each time step $t \in \{1, 2, \dots, T\}$, we encode frame I_t using the slow network if it’s a keyframe and the fast network otherwise. In our implementation, we use ResNet-101 as the slow network and ResNet-18 as the fast network. The encoder is shared among all tasks. We use $Slow(I_t)$ to denote features encoded by the slow network and $Fast(I_t)$ for features encoded by the fast network.

At the decoder step, we perform predictions on each task with a task-specific decoder $\{D_1, D_2, \dots, D_M\}$, where M is the total number of tasks. Each task-specific decoder consists of squeeze-excitation (SE) blocks on top of shared features from the encoder, inter-frame local attention (ILA) modules to extract and propagate task-specific features across frames and a set of conv layers. In order to fully leverage temporal information, we enable multi-frame feature propagation: a non keyframe receives features propagated from the last keyframe and the last non keyframe; a keyframe receives features propagated from the last non keyframe. This is different from existing attention-based feature propagation [21, 26] which only propagate features from a keyframe to a non-key frame.

3.2. Inter-frame Local Attention

The key challenge for attention based feature propagation is how to leverage inter-frame temporal cues to propagate features effectively and efficiently. We introduce a light-weight inter-frame local attention (ILA) module for feature propagation. As illustrated in Figure 3, ILA computes local attention weights W from the feature maps of two different frames (either two neighboring frames or a non keyframe and a keyframe) to exploit local motion changes.

Given a pair of frames I_t and I_k , ILA operates on feature maps f_t and f_k and propagates features from f_t to f_k . In our design (see Figure 3), the feature maps are the output of squeeze-and-excitation (SE) blocks. For each pixel on the feature map f_k , we propagate the features from f_t based on a weighted combination of pixels in a local neighborhood.

$$f_{t \rightarrow k}(i, j) = \sum_{x=-L/2}^{L/2} \sum_{y=-L/2}^{L/2} W_{i,j}(x, y) f_t(i+x, j+y) \quad (1)$$

where (i, j) denotes the pixel location in the image, L is the window size and W is the attention weight obtained by measuring the similarity between the two feature maps f_t and f_k . The attention weight matrix W is defined in the

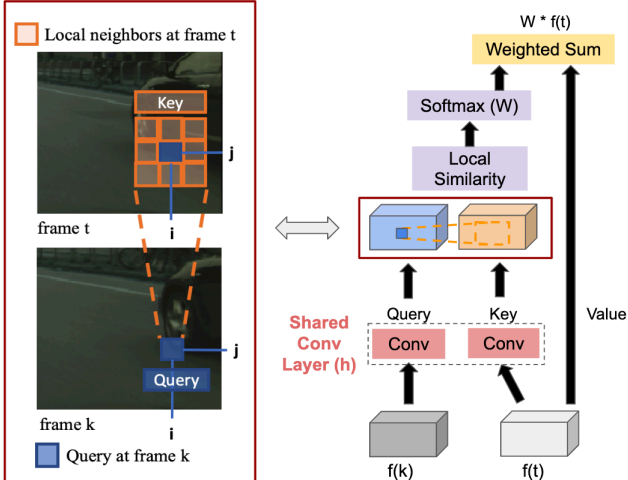


Figure 3: An illustrations of our inter-frame local attention (ILA). ILA is designed to account for motion by finding local attention weights in inter-frames. With a shared conv layers, our module generates high attention weighs on the similar features between frames.

following:

$$W_{i,j}(x, y) = \text{softmax}(h(f_k(i, j)) \cdot h(f_t(i + x, j + y))) \quad (2)$$

where $W_{i,j}(x, y)$ is the attention weight which measures the similarity between features at position (i, j) and $(i+x, i+y)$ of the two feature maps, respectively. Similar features should have higher attention weight. h is a 3×3 convolution layer shared between the two feature maps to capture the semantic information in a local window around pixel (i, j) . We use inner product to capture the similarities. Then a softmax layer is applied to ensure the sum of weights equals to 1. Note that ILA is performed only on local neighborhoods, resulting in reduced computational cost as compared to existing global attention modules [11]. It also helps achieve fast convergence by filtering out irrelevant pixels out of the local neighborhood.

Task-specific Attention. A common challenge in multi-task learning is on how to balance the task-share and task-specific features. A heavily shared representation provides benefit of reducing computational costs and helps prevent over-fitting, but is also shown to potentially hurt the accuracy due to limited model capacity to handle multiple different tasks [29]. To solve this issue, methods that add extra task specific layers to the multi-task network [27, 30, 32] gained popularity during the recent years and achieved better accuracy. However, the complex task-specific layers also increase computational burden significantly.

Our ILA module is task-specific, in order to learn discriminative task-specific features. In contrast to the previ-

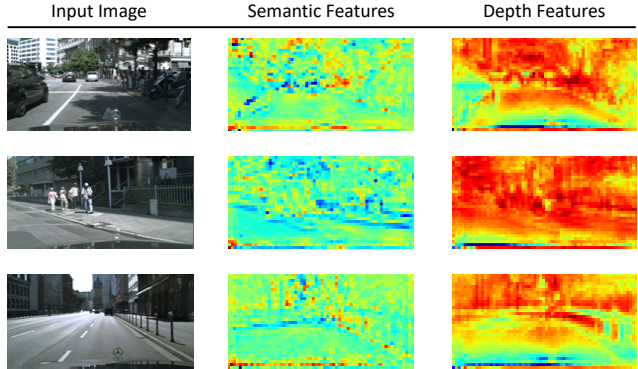


Figure 4: Visualization of task-specific features from our task-specific attention module.

ous works, ILA learns to select and propagate features from previous frames rather than from the backbone. Leveraging temporal information drastically reduces the required complexity of task-specific layers as the model capacity and discriminative power are shared across multiple frames. The other effective design is ILA only attends to features within a local window from previous frames. This assumption on temporal consistency reduces the computational cost of ILA. Compared to state-of-the-art attention-based multi-task network [27], our method achieves better accuracy with 54% reduction of FLOPs.

Visualization of the learned task-specific features are shown in Figure 4. We can see clear differences in feature patterns for different tasks. Semantic segmentation features highlight object patches, lines and boundaries, while the depth features highlight foreground and background. This confirms the effectiveness of ILA as a feature selector to focus on parts that are discriminative for each task.

3.3. Training with Adversarial Loss

Our local attention module assumes similar features propagate across frames. The high-level idea is similar to optical flow which assumes color constancy between pixels in consecutive images in order to capture motion. However, different backbones (e.g. ResNet-101 and ResNet-18) from the *Slow* and *Fast* branches cannot guarantee learning similar features for similar image patches, which could harm our attention based feature propagation.

We adopt adversarial learning to train the network to learn similar features between the *Slow* and *Fast* network. We leverage ideas used in GANs [16] where a discriminator D is trained to classify whether the features are output of the *Slow* network or the *Fast* network, and the *Fast* network is trained to confuse the discriminator by "mimicking" the output features of the *Slow* network. In practice, we observed combining $L1$ loss with the adversarial loss lead to improved accuracy. Our loss function \mathcal{L} is defined in the

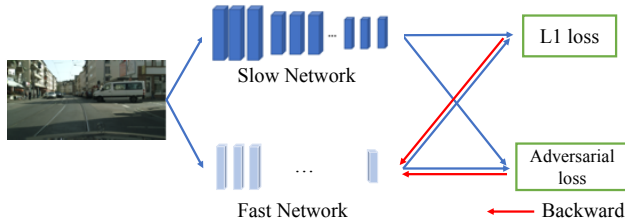


Figure 5: Adversarial learning. In order to let our attention module (ILA) capture temporal consistency, we adopt an adversarial learning strategy for training, where we use a combination of L1 and adversarial loss for the *Fast* network to mimic the features learned by the *Slow* network.

following:

$$\begin{aligned} \mathcal{L} &= \min(\alpha \mathcal{L}_{L1} - \beta \min_D \mathcal{L}_{adversarial}) \\ \mathcal{L}_{L1} &= |Slow(I_t) - Fast(I_t)| \\ \mathcal{L}_{adversarial} &= \log D(Slow(I_t)) + \log(1 - D(Fast(I_t))) \end{aligned} \quad (3)$$

where $Slow(I_t)$ and $Fast(I_t)$ are the features of the *Slow* and *Fast* backbone networks on image I_t . The loss function L enforces the *Fast* network to mimic the features learned from the *Slow* network.

4. Experiments

We validate our approach in the following two aspects for both accuracy and computation cost. (1) Comparison with the state-of-the-art approaches for multi-task learning on videos, and the ablation study for our proposed task-specific attention module and the adversarial loss. (2) The efficacy of our attention based feature propagation approach compared with other feature propagation methods.

4.1. Implementation Details

We implement our network using PyTorch. We train our network using ADAM optimizer with $\beta_1 = 0.9$ and $\beta_2 = 0.99$. The learning rate is $1e^{-4}$ and batch size is 4. The training loss converges after 50 epochs. For the adversarial loss in Equ 3, we set $\alpha = \beta = 1$. Our local attention module computes on a window size of $L = 5$ in Equ. 2. We use DeepLab-ResNet101 [3, 28, 18] as a *Slow* network and DeepLab-ResNet18 as a *Fast* Network. The backbones are pre-trained on ImageNet [6] and finetuned for multi-task learning. For brevity, Deeplab-ResNet101 is denoted as D101. D101-18 refers to the slow-fast network with DeepLab-ResNet101 and DeepLab-ResNet18. Each task-specific decoder consists of three convolution layers with kernel size of 3x3, 1x1 and 1x1 respectively, and feature size of 512 and 256 in between. To compare our atten-

tion based feature propagation with other feature propagation methods, we directly train our network for the single task of semantic video segmentation.

Keyframe Interval. We train our network with a fixed keyframe interval of $K = 5$ (every 5-th frame is a keyframe). For evaluation, since frames in a video are sparsely annotated (*e.g.*, 20-th frame in a video clip) in existing datasets, we measure performances of an annotated frame by running our method for all possible keyframe interval offsets $[0, K - 1]$ and report the averaged accuracy and GFLOPs. For the evaluation of feature propagation on semantic video segmentation, we use the fixed keyframe intervals of 5 and 10 for training respectively.

4.2. Setup

Datasets. We evaluate our method on two video datasets: Cityscapes [5] and NYUd v2 [34]. For evaluations on multi-task learning, we follow the evaluation protocols as in Liu *et al.* [27]: on Cityscapes, we perform 2 *task predictions* including 7-class segmentation and depth estimation, where images are resized to 256×512 to boost up training process; on the NYUd v2 dataset, we perform 3 *task predictions* including 13-class segmentation and depth estimation, with input images resized to 288×384 . In addition, we train our model on the single task of 19-class semantic video segmentation, and report the performance compared with Jain *et al.* [21].

Metrics. For semantic segmentation, we use mean intersection-over union (mIoU) metric and pixel accuracy (PA). For depth estimation, we evaluate on absolute and relative depth errors compared to the ground truth. For normal estimation, we measure the mean and median angle distances between the predicted angles and ground-truth angles. We also measure the percentage of pixels that are within the angles of 11° , 22.5° , 30° to the ground-truth. We compare on computation cost based on GFLOPs.

Baselines. We compare with state-of-the-art multi-task learning approaches: MTAN [27], Cross-Stitch network [30] and MultiNet++ [4]. MTAN and Cross-Stitch are single frame based, while MultiNet++ uses multi-frame as input. Since the original proposed MTAN and Cross-Stitch use different backbones, for fair comparison, we report performance of the two using the same DeepLab-ResNet101 backbone as ours (which shows better performance than using the backbone mentioned in their papers). We use the four outputs of each group of layers containing the residual blocks in the backbone as input for the attention modules for the two methods. For our method and MultiNet++, we use the slow-fast network with ResNet101 and ResNet18. Please refer to the supplementary for details.

We also compare with two other baselines: **D101-SingleTask**, which uses a separate ResNet101 backbone for training each task without any shared features; **D101-**

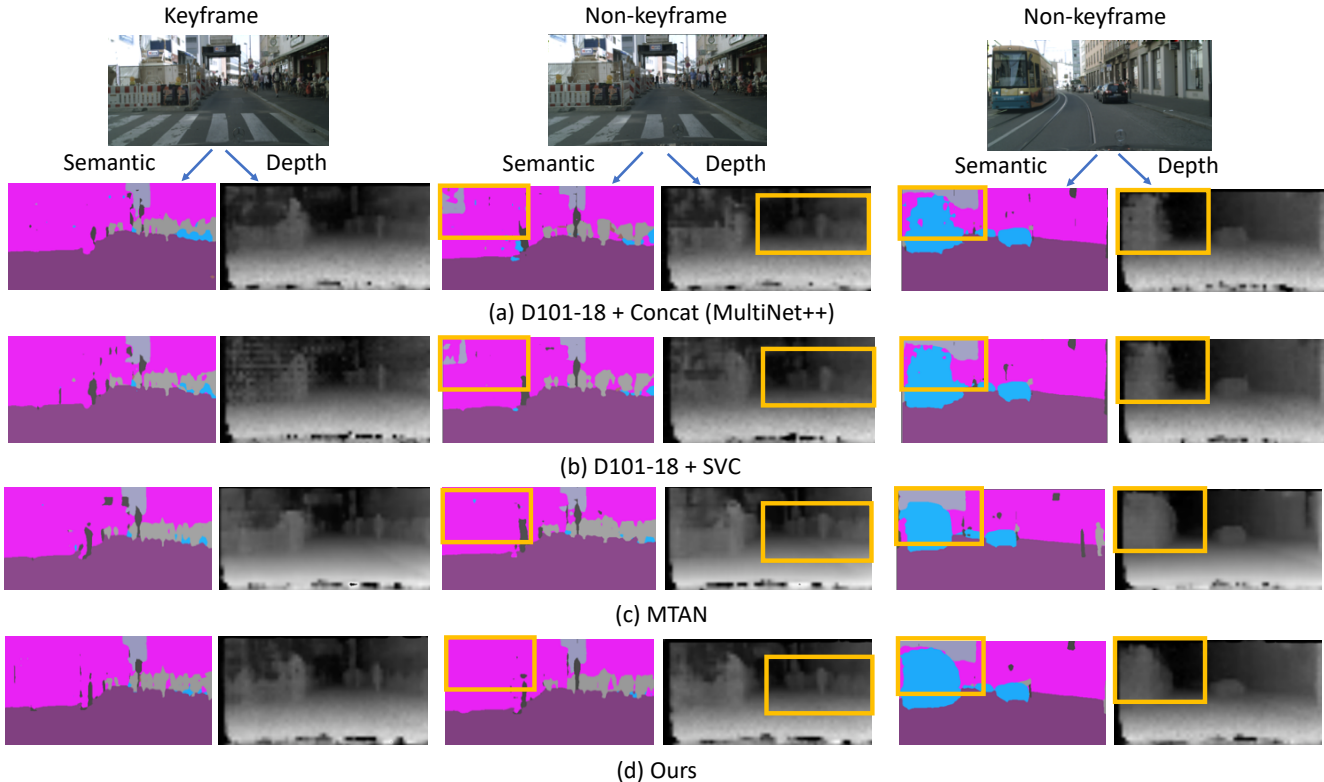


Figure 6: Qualitative results for video based multi-task learning on Cityscapes dataset. We choose the two frames in a video, where the first image is a key frame and the second image is non-keyframe with offset 4. For keyframe, the three methods produce very similar qualitative results. For non-keyframes, the baseline methods (a, b) performs worse (see orange boxes) but our method (b) still obtains robust to the non-keyframes. Our method is robust to non-keyframes.

MultiTask, which uses the shared ResNet101 backbone with task-specific decoders.

4.3. Video Based Multi-Task Learning

We report the performance of video based multi-task learning on the Cityscapes dataset in Table 1 and the NYUD v2 dataset in Table 2 respectively. We show in Figure 6 and Figure 7 sample qualitative results from each dataset. Please find more results in the supplemental.

In Table 1, our approach outperforms all other methods for depth estimation and achieves the the best accuracy for semantic segmentation, while ranking the 2nd for mIOU on Cityscapes. In Table 2, on the NYUD v2 dataset, we outperform other approaches for depth estimation and one metric of mIOU for semantic segmentation, with ranked 2nd segmentation accuracy. Our approach shows slightly worse performance for normal estimation than Cross-Stitch. This is because Cross-Stitch has task-specific backbones, while our model use a single shared one, which is significantly computationally efficient, saving 70% of computational costs (236 vs. 70 GFLOPs). We rank the 2nd for GFLOPs right after MultiNet++ but with much better accu-

Model	Segmentation		Depth		GFLOPs
	mIOU \uparrow	Acc. \uparrow	Abs. \downarrow	Rel. \downarrow	
D101-SingleTask	63.9	94.4	1.02	25.3	187
D101-MultiTask	63.8	94.4	1.06	31.9	93
MTAN-SegNet [27]	53.0	91.1	1.44	33.6	168
MTAN *	64.2	94.5	1.06	26.3	161
Cross-Stitch*	64.5	94.5	1.04	33.0	187
MultiNet++ [4]	61.6	93.9	1.08	28.5	47
Ours w/o MF&TS	63.8	94.4	1.05	32.9	48
Ours w/o TS	64.1	94.5	1.03	31.5	55
Ours	64.3	94.6	1.02	25.2	70

Table 1: Comparison for video based multi-task learning on the Cityscapes dataset. * means training with the same Deeplab-ResNet101 backbone. Ours and MultiNet++ uses the D101-18 backbone.

racy.

Ablation study. The last three rows in Table 1 show the ablation study of our method. “ours w/o TS” means our approach without task-specific attention design. “ours w/o MF&TS” means without both task-specific design and fea-

Model	Segmentation		Depth		Normal Estimation					GFLOPs
					Angle Dist. ↓		Angle° Within ↑			
	mIOU ↑	Acc. ↑	Abs. ↓	Rel. ↓	Mean	Median	11.25°	22.5°	30.0°	
D101-SingleTask	37.2	75.0	39.3	16.6	22.8	16.6	35.7	62.8	73.9	236
D101-MultiTask	37.1	75.3	39.0	16.3	23.7	17.6	34.0	60.2	71.7	79
MTAN-SegNet [27]	17.7	55.3	59.0	25.8	31.4	25.4	23.2	45.7	57.6	178
Cross-Stitch-SegNet [27]	14.7	50.2	64.8	28.7	33.6	28.6	20.1	40.5	52.0	213
MTAN*	37.1	74.3	40.0	16.9	23.9	18.1	33.5	59.5	70.4	151
Cross-Stitch*	37.5	74.5	39.5	16.2	22.7	16.5	36.8	63.0	73.8	236
MultiNet++* [4]	32.8	73.1	41.1	17.3	24.4	18.1	33.4	58.9	70.2	40
Ours	38.1	75.1	38.6	16.1	23.2	17.0	35.4	61.8	72.5	70

Table 2: Comparisons for video based Multi-task learning on NYUD v2 dataset. * means training with the same Deeplab-ResNet101 backbone as ours. D101 denotes the Deeplab-ResNet101 backbone. Cross-stitch* shows better results in the normal estimation task mostly because it contains task-specific backbones.

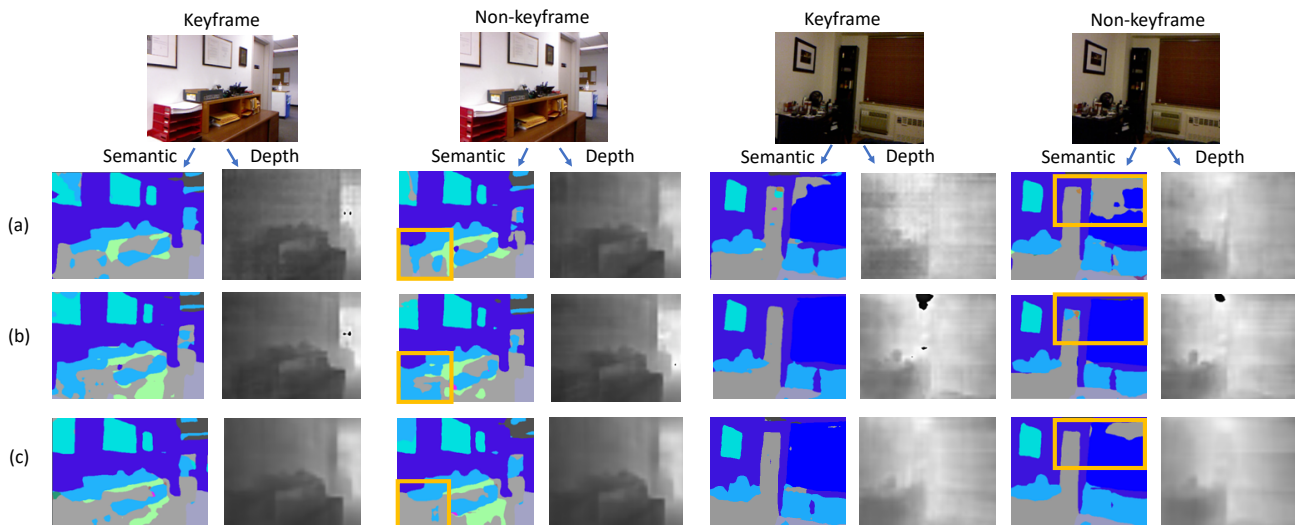


Figure 7: Qualitative results for multi-task learning on videos on the NYUD v2 dataset. We show comparison between (a) MultiNet++, (b) MTAN and (c) ours. Similar to 6, MultiNet++ performs worse on the non-keyframe.

Backbone	Adversarial	ILA	mIOU (↑)	Depth Err. (↓)
D101-18			61.6	1.08
D101-18	✓		61.8	1.07
D101-18		✓	61.9	1.08
D101-18	✓	✓	63.8	1.05

Table 3: Ablation study on our ILA module. ILA combined with adversarial learning lead to clear improvement.

Backbone	Window Size	mIOU (↑)	Depth Err. (↓)
D101-18	3x3	64.1	1.02
D101-18	5x5	64.3	1.02
D101-18	7x7	64.2	1.02
D101-18	Global	62.4	1.10

Table 4: Ablation study on the kernel size in ILA module. ILA performs better than global attention in multi-task learning.

ture propagation for neighboring frames. Our full approach shows the best performed accuracy with a small increase in FLOP.

We also show our ablation study on our inter-frame local attention (ILA). First, Table 3 reports the impact of the adversarial loss (eq. 3). In the third line of Table 3, it shows that the ILA alone does not greatly improve the performances. However, when ILA is combined with the ad-

versarial loss, it significantly increases the performance. In addition, we show the ablation study for the local window size in Table 4. ILA is not sensitive to small changes in the window size, but the performance drops significantly when the window size is global.

Weighting Strategies. In the above experiments, we use the equal weighting for each task. In Table 5, we show per-

Backbone	Weighting	mIOU (\uparrow)	Depth Err. (\downarrow)
D101-18	Equal	64.3	1.02
D101-18	Uncertainty [22]	64.3	1.01
D101-18	DWA [27]	64.2	1.02

Table 5: Different weighting strategies for multi-task learning. Our method is not sensitive to the weighting strategies.

Backbone	K	Feature Prop.	mIOU (%)
D101-50	5	Optical flow	74.2
D101-50	5	ILA (Ours)	75.1
D101-50	10	Optical flow	72.9
D101-50	10	ILA (Ours)	74.8

Table 6: Comparison with optical-flow based feature propagation [21] for the semantic segmentation task on Cityscapes. A keyframe interval is denoted by K .

Feature Prop.	Segmentation		Depth	
	mIOU \uparrow	Acc. \uparrow	Abs. \downarrow	Rel. \downarrow
(a) Cityscapes				
SVC [26]	62.3	94.0	1.06	33.3
ILA (Ours)	63.8	94.4	1.05	32.9
(b) NYUv2				
SVC [26]	35.7	74.7	40.3	17.0
ILA (Ours)	36.6	74.8	39.2	16.5

Table 7: Comparison with for feature propagation methods with D101-18 backbone on Cityscapes and NYUv2

formance with different weighting strategies for the multi-tasks: Uncertainty Weighting [22] and Dynamic Weight Average [27]. These weighting strategies are proposed to find a balance between different tasks, since a model can be biased to a certain task. A desired multi-task learning model should not depend on these weighting schemes, so that the model itself can find a proper balance between tasks. We observe that our method achieves the similar performance on different weighting strategies and thus is not sensitive to the weighting schemes.

4.4. Comparisons on Feature Propagation

We compare our attention based feature propagation with the two methods:(1) optical flow based warping with FlowNet-S [8], which shows state-of-the-art performance on the single task of semantic video segmentation for the Accel method [21] and (2) spatially variant [26] (SVC) also for semantic video segmentation. We use the same backbone for all methods for fair comparisons.

Performance comparison. To compare with optical-flow based warping [21], we follow their semantic segmentation evaluation protocol as shown in Table 6. Feature propagated with ILA obtains higher accuracy than the

Feature Propagation	GFLOPs	# Conv.	# Param
(a) Input size: 258×512			
Optical flow [21, 8]	7.5	23	38M
SVC [26]	5.4	3	3M
ILA (Ours)	0.2	1	0.2M
(b) Input size: 1024×2048			
Optical flow [21, 8]	71.2	23	38M
SVC [26]	108	3	3M
ILA (Ours)	5.4	1	0.2M

Table 8: Comparison on feature propagation modules. SVC represents the method of [26]. Our method is light-weight and computationally efficient.

method based on optical flow warping [21]. We observe that the accuracy improvements of our method are more evident in the higher keyframe interval.

In Table 7, we provide comparisons with [26] on Cityscapes and NYUd v2 on multi-task learning. Our method outperforms other method in the two datasets with less computational burden. We observe that the quality of optical-flow estimation is bad in this evaluation protocol (*i.e.*, low-resolution images), so the optical flow warping based feature propagation performs worse.

Space and computation cost. In Table 8, we show the comparison of GFLOPs, number of convolutional layers and number of parameters for the optical flow warping, SVC and our inter-frame local attention module (ILA). report numbers given different input sizes. ILA consists of only one convolutional layers, making it much more memory efficient than the other two methods. For GFLOPs, other methods require more computational burden than our method and the gain is more evident when the input size is larger.

5. Conclusion

We present an efficient and effective multi-task learning framework on video streams. We propose a novel task-specific inter-frame local attention (ILA) module, which accounts for motion and propagate discriminative task-specific features over time in a spatial-variant manner. Our attention module is much faster, more accurate, and modular compared to prior feature propagation methods. We also show that the inter-frame local attention module can be used to extract task-specific features with minimal computation. Our experiments show that our method significantly reduces the computational cost without compromising accuracy compared to the state-of-the-art multi-task learning models.

References

- [1] Kai Chen, Jiangmiao Pang, Jiaqi Wang, Yu Xiong, Xiao-xiao Li, Shuyang Sun, Wansen Feng, Ziwei Liu, Jianping Shi, Wanli Ouyang, et al. Hybrid task cascade for instance segmentation. In *Proceedings of the IEEE Conference on Computer Vision and Pattern Recognition*, pages 4974–4983, 2019. 2
- [2] Liang-Chieh Chen, Alexander Hermans, George Papandreou, Florian Schroff, Peng Wang, and Hartwig Adam. Masklab: Instance segmentation by refining object detection with semantic and direction features. In *Proceedings of the IEEE Conference on Computer Vision and Pattern Recognition*, pages 4013–4022, 2018. 2
- [3] Liang-Chieh Chen, George Papandreou, Iasonas Kokkinos, Kevin Murphy, and Alan L Yuille. Deeplab: Semantic image segmentation with deep convolutional nets, atrous convolution, and fully connected crfs. *IEEE transactions on pattern analysis and machine intelligence*, 40(4):834–848, 2017. 5, 10
- [4] Sumanth Chennupati, Ganesh Sistu, Senthil Yogamani, and Samir A Rawashdeh. Multinet++: Multi-stream feature aggregation and geometric loss strategy for multi-task learning. In *Proceedings of the IEEE Conference on Computer Vision and Pattern Recognition Workshops*, pages 0–0, 2019. 1, 2, 5, 6, 7, 10
- [5] Marius Cordts, Mohamed Omran, Sebastian Ramos, Timo Rehfeld, Markus Enzweiler, Rodrigo Benenson, Uwe Franke, Stefan Roth, and Bernt Schiele. The cityscapes dataset for semantic urban scene understanding. In *Proceedings of the IEEE conference on computer vision and pattern recognition*, pages 3213–3223, 2016. 2, 5
- [6] Jia Deng, Wei Dong, Richard Socher, Li-Jia Li, Kai Li, and Li Fei-Fei. Imagenet: A large-scale hierarchical image database. In *2009 IEEE conference on computer vision and pattern recognition*, pages 248–255. Ieee, 2009. 5
- [7] Yuntian Deng, Yoon Kim, Justin Chiu, Demi Guo, and Alexander Rush. Latent alignment and variational attention. In *Advances in Neural Information Processing Systems*, pages 9712–9724, 2018. 2
- [8] Alexey Dosovitskiy, Philipp Fischer, Eddy Ilg, Philip Hausser, Caner Hazirbas, Vladimir Golkov, Patrick Van Der Smagt, Daniel Cremers, and Thomas Brox. FlowNet: Learning optical flow with convolutional networks. In *Proceedings of the IEEE international conference on computer vision*, pages 2758–2766, 2015. 8
- [9] David Eigen and Rob Fergus. Predicting depth, surface normals and semantic labels with a common multi-scale convolutional architecture. In *Proceedings of the IEEE international conference on computer vision*, pages 2650–2658, 2015. 2
- [10] Christoph Feichtenhofer, Haoqi Fan, Jitendra Malik, and Kaiming He. Slowfast networks for video recognition. In *Proceedings of the IEEE International Conference on Computer Vision*, pages 6202–6211, 2019. 2, 3
- [11] Jun Fu, Jing Liu, Haijie Tian, Yong Li, Yongjun Bao, Zhiwei Fang, and Hanqing Lu. Dual attention network for scene segmentation. In *Proceedings of the IEEE Conference on Computer Vision and Pattern Recognition*, pages 3146–3154, 2019. 2, 4
- [12] Raghudeep Gadde, Varun Jampani, and Peter V Gehler. Semantic video cnns through representation warping. In *Proceedings of the IEEE International Conference on Computer Vision*, pages 4453–4462, 2017. 2
- [13] Yuan Gao, Jiayi Ma, Mingbo Zhao, Wei Liu, and Alan L Yuille. Nddr-cnn: Layerwise feature fusing in multi-task cnns by neural discriminative dimensionality reduction. In *Proceedings of the IEEE Conference on Computer Vision and Pattern Recognition*, pages 3205–3214, 2019. 1, 10
- [14] Rohit Girdhar, Joao Carreira, Carl Doersch, and Andrew Zisserman. Video action transformer network. In *Proceedings of the IEEE Conference on Computer Vision and Pattern Recognition*, pages 244–253, 2019. 2
- [15] Rohit Girdhar and Deva Ramanan. Attentional pooling for action recognition. In *Advances in Neural Information Processing Systems*, pages 34–45, 2017. 2
- [16] Ian J. Goodfellow, Jean Pouget-Abadie, Mehdi Mirza, Bing Xu, David Warde-Farley, Sherjil Ozair, Aaron C. Courville, and Yoshua Bengio. Generative adversarial nets. In *NIPS*, 2014. 4
- [17] Kaiming He, Georgia Gkioxari, Piotr Dollár, and Ross Girshick. Mask r-cnn. In *Proceedings of the IEEE international conference on computer vision*, pages 2961–2969, 2017. 2
- [18] Kaiming He, Xiangyu Zhang, Shaoqing Ren, and Jian Sun. Deep residual learning for image recognition. In *The IEEE Conference on Computer Vision and Pattern Recognition (CVPR)*, June 2016. 5, 10
- [19] Jie Hu, Li Shen, and Gang Sun. Squeeze-and-excitation networks. In *Proceedings of the IEEE conference on computer vision and pattern recognition*, pages 7132–7141, 2018. 2
- [20] Zilong Huang, Xinggang Wang, Lichao Huang, Chang Huang, Yunchao Wei, and Wenyu Liu. Ccnet: Criss-cross attention for semantic segmentation. In *Proceedings of the IEEE International Conference on Computer Vision*, pages 603–612, 2019. 2
- [21] Samvit Jain, Xin Wang, and Joseph E Gonzalez. Accel: A corrective fusion network for efficient semantic segmentation on video. In *Proceedings of the IEEE Conference on Computer Vision and Pattern Recognition*, pages 8866–8875, 2019. 1, 2, 3, 5, 8, 11
- [22] Alex Kendall, Yarin Gal, and Roberto Cipolla. Multi-task learning using uncertainty to weigh losses for scene geometry and semantics. In *Proceedings of the IEEE Conference on Computer Vision and Pattern Recognition*, pages 7482–7491, 2018. 1, 2, 8
- [23] Diederik P Kingma and Jimmy Ba. Adam: A method for stochastic optimization. *arXiv preprint arXiv:1412.6980*, 2014. 10
- [24] Iasonas Kokkinos. Ubernet: Training a universal convolutional neural network for low-, mid-, and high-level vision using diverse datasets and limited memory. In *Proceedings of the IEEE Conference on Computer Vision and Pattern Recognition*, pages 6129–6138, 2017. 2
- [25] Yanwei Li, Xinze Chen, Zheng Zhu, Lingxi Xie, Guan Huang, Dalong Du, and Xingang Wang. Attention-guided

unified network for panoptic segmentation. In *Proceedings of the IEEE Conference on Computer Vision and Pattern Recognition*, pages 7026–7035, 2019. 2

[26] Yule Li, Jianping Shi, and Dahua Lin. Low-latency video semantic segmentation. In *Proceedings of the IEEE Conference on Computer Vision and Pattern Recognition*, pages 5997–6005, 2018. 2, 3, 8, 11

[27] Shikun Liu, Edward Johns, and Andrew J Davison. End-to-end multi-task learning with attention. In *Proceedings of the IEEE Conference on Computer Vision and Pattern Recognition*, pages 1871–1880, 2019. 1, 2, 4, 5, 6, 7, 8, 10, 11

[28] Jonathan Long, Evan Shelhamer, and Trevor Darrell. Fully convolutional networks for semantic segmentation. In *Proceedings of the IEEE conference on computer vision and pattern recognition*, pages 3431–3440, 2015. 5

[29] Kevis-Kokitsi Maninis, Ilija Radosavovic, and Iasonas Kokkinos. Attentive single-tasking of multiple tasks. In *Proceedings of the IEEE Conference on Computer Vision and Pattern Recognition*, pages 1851–1860, 2019. 2, 4

[30] Ishan Misra, Abhinav Shrivastava, Abhinav Gupta, and Martial Hebert. Cross-stitch networks for multi-task learning. In *Proceedings of the IEEE Conference on Computer Vision and Pattern Recognition*, pages 3994–4003, 2016. 1, 2, 4, 5, 10

[31] David Nilsson and Cristian Sminchisescu. Semantic video segmentation by gated recurrent flow propagation. In *Proceedings of the IEEE Conference on Computer Vision and Pattern Recognition*, pages 6819–6828, 2018. 2

[32] Sebastian Ruder12, Joachim Bingel, Isabelle Augenstein, and Anders Søgaard. Latent multi-task architecture learning. In *AAAI*, 2019. 2, 4

[33] Ozan Sener and Vladlen Koltun. Multi-task learning as multi-objective optimization. In *Advances in Neural Information Processing Systems*, pages 527–538, 2018. 2

[34] Nathan Silberman, Derek Hoiem, Pushmeet Kohli, and Rob Fergus. Indoor segmentation and support inference from rgb-d images. In *European Conference on Computer Vision*, pages 746–760. Springer, 2012. 2, 5

[35] Marvin Teichmann, Michael Weber, Marius Zoellner, Roberto Cipolla, and Raquel Urtasun. Multinet: Real-time joint semantic reasoning for autonomous driving. In *2018 IEEE Intelligent Vehicles Symposium (IV)*, pages 1013–1020. IEEE, 2018. 2

[36] Ashish Vaswani, Noam Shazeer, Niki Parmar, Jakob Uszkoreit, Llion Jones, Aidan N Gomez, Łukasz Kaiser, and Illia Polosukhin. Attention is all you need. In *Advances in neural information processing systems*, pages 5998–6008, 2017. 2

[37] Sanghyun Woo, Jongchan Park, Joon-Young Lee, and In So Kweon. Cbam: Convolutional block attention module. In *Proceedings of the European Conference on Computer Vision (ECCV)*, pages 3–19, 2018. 2

[38] Dan Xu, Wanli Ouyang, Xiaogang Wang, and Nicu Sebe. Pad-net: Multi-tasks guided prediction-and-distillation network for simultaneous depth estimation and scene parsing. In *Proceedings of the IEEE Conference on Computer Vision and Pattern Recognition*, pages 675–684, 2018. 2

[39] Han Zhang, Ian Goodfellow, Dimitris Metaxas, and Augustus Odena. Self-attention generative adversarial networks. *arXiv preprint arXiv:1805.08318*, 2018. 2

[40] Xizhou Zhu, Yuwen Xiong, Jifeng Dai, Lu Yuan, and Yichen Wei. Deep feature flow for video recognition. In *Proceedings of the IEEE Conference on Computer Vision and Pattern Recognition*, pages 2349–2358, 2017. 1, 2

A. Experiment Details for Fair Comparison

As stated in Sec.4.2 in the main paper, for fair comparison to other methods (MTAN [27], Cross-Stitch [30] and MultiNet++ [4]), we unify the backbone for all method as Deeplab-ResNet101 [3, 18]. Note that after using Deeplab-ResNet101, the performance for MTAN, Cross-Stitch and MultiNet++ gets improved compared to their originally reported numbers as shown in Table 9. Deeplab-ResNet101 is initialized with pre-trained weights on ImageNet but decoders use randomly initialized weights. Then, the model is finetuned for multi-task learning.

For implementation details, since all multi-task learning models except Cross-Stitch use shared encoder, we pre-train a shared multi-task encoder based on Deeplab-ResNet101 for each method (named as “D101-MultiTask”). For the Cross-Stitch model we pre-train a task specific encoder (named as “D101-SingleTask”). Using networks pre-trained on multi-task learning shows better performances than just directly finetuning pre-trained weights on ImageNet [13]. We first train D101-SingleTask and D101-MultiTask with Adam optimizer with learning [23] rate $1e^{-4}$ for 120 epochs with a decay rate $1e^{-1}$ at every 40-th epoch. For our SlowFast based network, we use the D101-MultiTask for our slow network. We also train a D18-MultiTask for the *Fast* network with the same optimizer and training setting. For fair comparison with MultiNet++, we use the same pre-trained slow-fast network for MultiNet++, but concatenate neighboring frames as input to learn from videos as proposed in their paper.

Note that we also report in the main paper the performance comparison with our pre-trained “D101-SingleTask” and “D101-MultiTask”.

Model	Segmentation		Depth	
	mIOU ↑	Acc. ↑	Abs. ↓	Rel. ↓
MTAN-SegNet [27]	53.0	91.1	1.44	33.6
MTAN-ResNet101	64.2	94.5	1.06	26.3
Cross-Stitch-SegNet [27]	50.1	90.3	1.54	34.5
Cross-Stitch-ResNet101	64.5	94.5	1.04	33.0

Table 9: Comparison of different backbones. Using the ResNet101 backbone improves the accuracy.

B. Ablation on Adversarial Loss

We use the $L1$ loss and adversarial loss to learn similar features between the *Slow* and *Fast* network. In this section we further analyze the impact of adversarial loss on our full approach (D101-18 with ILA, multi-frame attention, and task-specific attention), as shown in Table 10. Please note that Table 3 in the main paper uses $L1$ loss and adversarial loss together. The adversarial loss can improve the performances on the semantic segmentation task.

Backbone	L1 loss	Adversarial	mIOU (\uparrow)	Depth Err. (\downarrow)
D101-18	✓		63.8	1.02
D101-18	✓	✓	64.3	1.02

Table 10: Ablation study on adversarial loss and $L1$ loss.

C. Analysis on GFLOPs

We measure GFLOPs using the “thop” library¹. Our ILA module uses a single shared 3×3 convolutional layer with channel dimensionality reduction rate of 16, so the number of channels of a key and a query is only 32. This reduction also helps reduce the number of computation needed to measure similarity between the key and query even when the input size is large.

We draw conclusions for our GFLOPs improvements in the abstract and introduction section based on Tables 2 and 8 in the main paper. As shown in the Table 8 in the main paper, our features propagation takes only 4% (0.2/5.4 GFLOPs) of computations in the SVC feature propagation [26]. When compared with the state-of-the-art multi-task learning methods, our model reduces **70%** (70/236 GFLOPs) of the computations in the Cross-Stitch [27] and **46%** (60/151 GFLOPs) of MTAN [27] as shown in Table 2.

D. Detailed Comparison for Feature Propagation

In Table 11, we provide more detailed comparisons between our attention based feature propagation and the optical flow based feature warping method by Jain *et al.* [21]. We compare the task of video semantic segmentation as in [21]. Our method outperforms [21], and is more robust to different keyframe interval. Note that we only apply our ILA module for fair comparison with other feature propagation methods (*i.e.* without multi-frame and task-specific attention).

E. Ablation for *Slow* network-only

We apply our full feature propagation method (inter-frame local attention (ILA) + multi-frame feature propaga-

Backbone	K	Feature Prop.	mIOU (%)
D101-18	5	Optical flow	72.1
D101-18	5	ILA (Ours)	73.2
D101-18	10	Optical flow	69.8
D101-18	10	ILA (Ours)	72.1
D101-34	5	Optical flow	72.4
D101-34	5	ILA (Ours)	74.3
D101-34	10	Optical flow	70.1
D101-34	10	ILA (Ours)	73.8

Table 11: Supplements to Table 6 in the main paper. Comparison with optical-flow based feature propagation [21] for the semantic segmentation task on Cityscapes. A keyframe interval is denoted by K . We show detailed comparison using different backbones and keyframe intervals.

tion + task specific) on *Slow* network-only model. This means that the keyframe interval is 1. Table 12 shows the results on Cityscapes. In all cases, using our feature propagation method shows significant improvements on the depth estimation task.

Model	Segmentation		Depth	
	mIOU \uparrow	Acc. \uparrow	Abs. \downarrow	Rel. \downarrow
D101-Multi	63.8	94.4	1.06	31.9
D101-Multi + Ours	64.4	94.6	1.02	25.8
D50-Multi	63.1	94.2	1.09	33.0
D50-Multi + Ours	63.3	94.5	1.02	25.1
D18-Multi	60.3	93.4	1.21	34.8
D18-Multi + Ours	61.5	93.8	1.07	25.8

Table 12: Evaluation of a Slow-only network with our task-specific inter-frame local attention (ILA) module on Cityscapes.

¹<https://github.com/Lyken17/pytorch-OpCounter>